Standard Model precision measurements
Misure di precisione del modello standard

Lesson 2: Asymmetries at Z pole

Stefano Lacaprara

INFN Padova

Dottorato di ricerca in fisica
Università di Padova, Dipartimento di Fisica e Astronomia
Padova, 7 March 2019

Outline

Outline

Outline

Input to global EWK fit

(in parenthesis the order followed in these lessons)

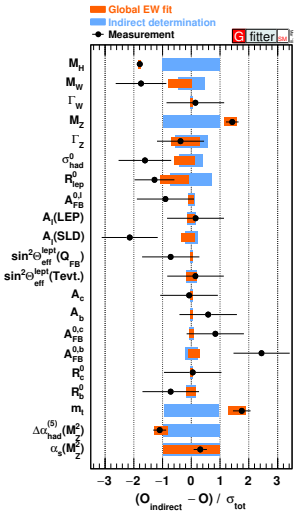

- Higgs mass (5)
  - LHC
- W mass and width (3)
  - LEP2, Tevatron, LHC
- Z-pole observables (1,2)
  - LEP1, SLD
  - M_Z, Γ_Z
  - σ_0^{had}
  - $\sin^2\theta^{lept}_{eff}$
  - Asymmetries
  - BR $R^0_{lep,b,c} = \Gamma_{had}/\Gamma_{\ell\ell,b\bar{b},c\bar{c}}$
- Top mass (4)
  - Tevatron, LHC
- other:
  - $\alpha_s(M_Z^2)$, $\Delta\alpha_{had}(M_Z^2)$

Input to global EWK fit
(in parenthesis the order followed in these lessons)

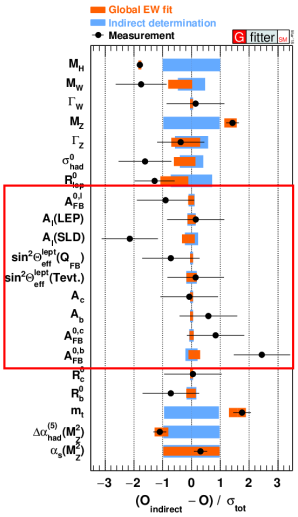

- Higgs mass (5)
  - LHC
- W mass and width (3)
  - LEP2, Tevatron, LHC
- Z-pole observables (1,2)
  - LEP1, SLD
  - M_Z, Γ_Z
  - σ^{had}_0
  - $\sin^2\theta^{lept}_{eff}$
  - Asymmetries
  - BR $R^0_{lep,b,c} = \Gamma_{had}/\Gamma_{\ell\ell,b\bar{b},c\bar{c}}$
- Top mass (4)
  - Tevatron, LHC
- other:
  - $\alpha_s(M^2_Z)$, $\Delta\alpha_{had}(M^2_Z)$

Cross section for $e^+e^- \rightarrow \mu^+\mu^-$ at LEP I

$$\frac{d\sigma}{d\cos\theta} = \frac{\pi\alpha^2}{2s}\left[F_\gamma(\cos\theta) + F_{\gamma Z}(\cos\theta)\frac{s(s-M_Z^2)}{(s-M_Z^2)^2+M_Z^2\Gamma_Z^2} + F_Z(\cos\theta)\frac{s^2}{(s-M_Z^2)^2+M_Z^2\Gamma_Z^2}\right]$$

γ | γ/Z interference | Z

vanishes at $\sqrt{s} \approx M_Z$

$$F_\gamma(\cos\theta) = Q_e^2 Q_\mu^2 (1+\cos^2\theta) = (1+\cos^2\theta)$$

$$F_{\gamma Z}(\cos\theta) = \frac{Q_e Q_\mu}{4\sin^2\theta_W\cos^2\theta_W}[2g_V^e g_V^\mu(1+\cos^2\theta) + 4g_A^e g_A^\mu\cos\theta]$$

$$F_Z(\cos\theta) = \frac{1}{16\sin^4\theta_W\cos^4\theta_W}[(g_V^{e^2}+g_A^{e^2})(g_V^{\mu^2}+g_A^{\mu^2})(1+\cos^2\theta) + 8g_V^e g_A^e g_V^\mu g_A^\mu\cos\theta]$$

Asymmetries [1]

The key features of the SM x-section for $ee \to f\bar{f}$ production can be fully exploited by looking at the **differential x-section** $\frac{d\sigma}{d\cos\theta}$ as well as to effects related to the **helicities of the fermions** in the initial or final state.

Both are related to the parity violation present in the neutral current of the SM lagrangian.

Possible asymmetries

- $\frac{d\sigma}{d\cos\theta}$: Forward-backward asymmetry A_{FB} (LEP);
- Helicity state: Left-Right asymmetry A_{LR} (initial state: SLD, final state:LEP [τ]);
- Both: Left-Right Forward-Backward asymmetry A_{LRFB} SLD;

We can differentiate the vector- and axial-vector coupling of the Z, including the measurement of $\sin\theta^{eff}_{W}$

From Z-lineshape we got [2]

$\sigma(s) = 12\pi \frac{\Gamma_e \Gamma_{had}}{M_Z^2} \frac{s}{(s-M_Z^2)^2 + M_Z^2 \Gamma_Z^2}$: At peak: $\sigma_0 = \frac{12\pi}{M_Z^2} \frac{\Gamma_e \Gamma_{had}}{\Gamma_Z}$

$\Gamma_{had} = \Sigma_{q \neq t} \Gamma_{q\bar{q}}$, and $\Gamma_Z = \Gamma_{ee} + \Gamma_{\mu\mu} + \Gamma_{\tau\tau} + \Gamma_{had} + \Gamma_{inv}$

So we measure the SM prediction for the total coupling of Z to fermions, but not the actual, inner form of the V-A strucutre

$$-i \frac{g}{\cos\theta_W} \gamma_\mu \frac{1}{2} \left(c_V^f - c_A^f \gamma^5 \right) \quad , \quad c_V^f = \left(T^3 - 2Q \sin^2\theta_W \right) \quad , \quad c_A^f = T^3$$

fermion	Q^f	T^3	c_A^f	c_V^f
$(\nu_e, \nu_\mu, \nu_\tau)_L$	0	1/2	1/2	$1/2 = 0.50$
$(e, \mu, \tau)_L$	-1	-1/2	-1/2	$-1/2 + 2\sin^2\theta_W = 0.03$
$(e, \mu, \tau)_R$	-1	0	0	$+2\sin^2\theta_W = 0.47$
$(u, c, t)_L$	2/3	1/2	1/2	$1/2 + 4/3\sin^2\theta_W = 0.19$
$(u, c, t)_R$	2/3	0	0	$4/3\sin^2\theta_W = 0.31$
$(d, s, b)_L$	-1/3	-1/2	-1/2	$-1/2 + 2/3\sin^2\theta_W = 0.34$
$(d, s, b)_R$	-1/3	0	0	$2/3\sin^2\theta_W = 0.16$

At $\sqrt{s} = M_Z$ the dominating term is the Z exchange.

Absorbing QED correction into effective coupling, and ignoring fermion masses, QCD ISR/FSR, ...

$$\frac{d\sigma}{d\cos\theta} = \frac{16\pi Q_f(N_c)}{2s}|\chi(s)|^2 \left((g_{Ve}^2 + g_{Ae}^2)(g_{Vf}^2 + g_{Af}^2)(1+\cos^2\theta) + 8 g_{Ve} g_{Ae} g_{Vf} g_{Af} \cos\theta\right)$$

Where lineshape is

$$\chi(s) = \frac{G_F M_W^2}{8\pi\sqrt{2}} \frac{s}{s - M_Z^2 + is\Gamma_Z/M_Z}$$

g_{Vf} (g_{Af}) are effective vector (axial) coupling of Z to fermion f.

At tree level, in S:

$c_{Af} = (T^{(3)})$, $c_{Vf} = (T^{(3)} - 2Q_f \sin^2\theta_W)$

A_{FB} definition

Definition

Forward-Backward asymmetry as

$$A_{FB} = \frac{\sigma_F - \sigma_B}{\sigma_F + \sigma_B} = \frac{N_F - N_B}{N_F + N_B}$$

where $F(B)$ is the direction of the final state fermion $(e^-, \mu^-, \tau^-, b, c)$ with respect to the incoming e^- beam

$$\sigma_{F(B)} = \int_{0(-1)}^{1(0)} \frac{d\sigma}{d\cos\theta} d\cos\theta$$

Modulo asymmetries in the detector acceptances and efficiencies,

$$\sigma_{F/B} \propto N_{F/B}$$

$$\frac{d\sigma}{d\cos\theta} = \frac{16\pi Q_f(N_c)}{2s}|\chi(s)|^2 \\ \left((g_{Ve}^2 + g_{Ae}^2)(g_{Vf}^2 + g_{Af}^2)(1+\cos^2\theta) + 8 g_{Ve} g_{Ae} g_{Vf} g_{Af} \cos\theta\right)$$

From $\frac{d\sigma}{d\cos\theta}$, and integrating over the angles

$\sigma_F - \sigma_B \propto \int_0^1 \cos\theta d\cos\theta - \int_{-1}^0 \cos\theta d\cos\theta = 1$

$\sigma_F + \sigma_B \propto \int_{-1}^1 (1+\cos^2\theta) d\cos\theta = 8/3$

$$A_{FB}^f = \frac{8 g_{Ve} g_{Ae} g_{Vf} g_{Af}}{8/3 (g_{Ve}^2 + g_{Ae}^2)(g_{Vf}^2 + g_{Af}^2)} \\ = \frac{3}{4}\left(\frac{2 g_{Ve} g_{Ae}}{g_{Ve}^2 + g_{Ae}^2}\right)\left(\frac{2 g_{Vf} g_{Af}}{g_{Vf}^2 + g_{Af}^2}\right) \\ = \frac{3}{4}\mathcal{A}_e \mathcal{A}_f$$

Alternative

One can rewrite the x-section as:

$$\begin{aligned}\frac{d\sigma}{d\cos\theta} =& \frac{16\pi Q_f(N_c)}{2s}|\chi(s)|^2 \\ & \left((g_{Ve}^2+g_{Ae}^2)(g_{Vf}^2+g_{Af}^2)(1+\cos^2\theta)+8g_{Ve}g_{Ae}g_{Vf}g_{Af}\cos\theta\right) \\ & \propto \left((1+\cos^2\theta)+8\frac{g_{Ve}g_{Ae}g_{Vf}g_{Af}}{(g_{Ve}^2+g_{Ae}^2)(g_{Vf}^2+g_{Af}^2)}\cos\theta\right) \\ & \propto \left((1+\cos^2\theta)+2\mathcal{A}_e\mathcal{A}_f\cos\theta\right) \\ & \propto \left((1+\cos^2\theta)+\frac{8}{3}A_{FB}\cos\theta\right)\end{aligned}$$

A_{FB} from counting experiment $A_{FB}=\frac{N_F-N_B}{N_F+N_B}$ **or** via a fit to the differential cross section $\frac{d\sigma}{d\cos\theta}\propto\left((1+\cos^2\theta)+\frac{8}{3}A_{FB}\cos\theta\right)$ via $\mathcal{L}$ fit.

The fit assumes SM for $\cos\theta$ distribution, so it is more model-dependent but has lower statistical error

$\frac{d\sigma}{d\cos\theta}$ in $\mu\mu$ channel

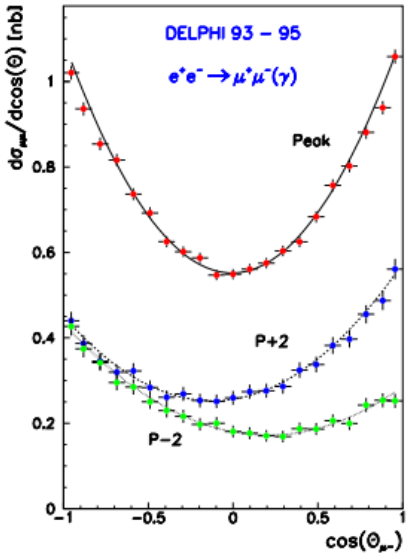

- On-peak (M_Z) and $\pm 2GeV$ off-peak
- As described before, there are two contributions:
  - $\propto (1 + \cos^2\theta)$ symmetical
  - $\propto \cos\theta$ gives asymmetry
- the asymmetry is **small**
  - $A_{FB} \propto g_V^f$ which is small for lepton. $c_V^f \approx 0.03$
- dependence of $\frac{d\sigma}{d\cos\theta}$ on $\sqrt{s}$
  - at $\sqrt{s} = M_Z^2$, resonance function is $\approx \frac{s}{s - M_Z^2}$
  - off-peak, the contribution from $\gamma - Z$ interference term does not vanish and so the actual shape changes

$\frac{d\sigma}{d\cos\theta}$ in *ee* channel

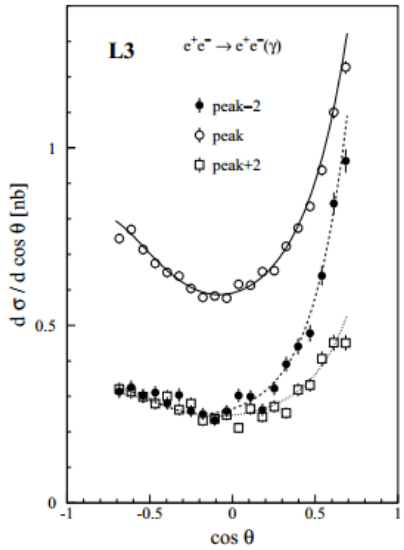

- Shape is different wrt to $\mu\mu$ due to presence of t-channel in *ee* final state.
- most of asymmetry comes from t-channel
- and s/t-channel interference off-peak

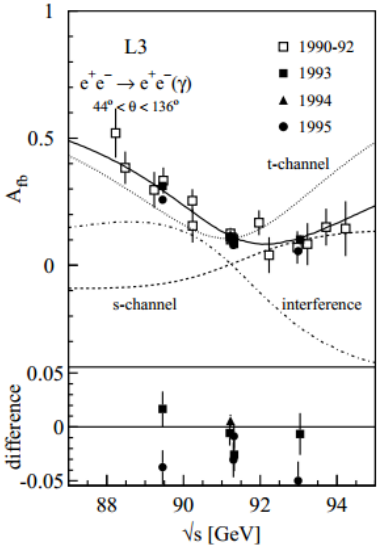

A_{FB} for ee channel wrt s

- Interference contribution vanishes (only) on-peak;
- it is dominant off-peak
  - $A_{FB} \propto g_{Ae} g_{Af} \frac{s(s-M_Z^2)}{(s-M_Z^2)^2+M_Z^2\Gamma_Z^2}$
- t-channel is important (for ee),
- s-channel is small;
  - in particular on-peak, since:
    - $A_{FB} \propto g_{Ve} g_{Ae} g_{Vf} g_{Af}$
    - g_{Vf} is small, expecially for leptons;
    - $g_{Ve,\mu} \sim 0.038$;

Corrections

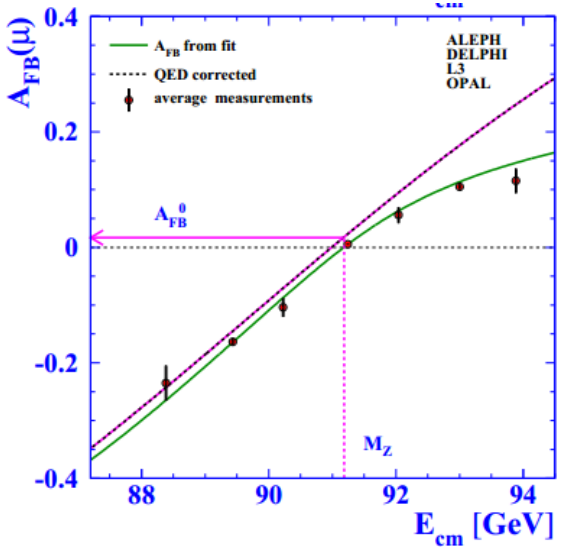

- As usual, the measured quantities suffers from large corrections: QED (ISR/FSR), self-energy, etc.
- Use pseudo-observable A_{FB}^0 (QED correction accounted for)
- Other correction (QCD, top, Higgs, ...) still there.

$\mathcal{A}_f$ in Standard Model

$\mathcal{A}_f$ depends on the vector- and axial-vector coupling of fermion to the Z.

$$\mathcal{A}_f = \frac{2 g_{Vf} g_{Af}}{g_{Vf}^2 + g_{Af}^2} = 2 \frac{g_{Vf}/g_{Af}}{1 + (g_{Vf}/g_{Af})^2}$$

In particular, it is strictly **null** if no axial/vector coupling exists for the neutral current.

Coupling SM: $c_{Vf} = (T^3 - 2Q_f \sin^2\theta_W)$ and $c_{Af} = (T^3)$

Using effective SM quantities, the radiative correction are re-absorbed
$\sin\theta^f_{W,eff} = (1 + \Delta\rho) \sin\theta^f_W$ with $\Delta\rho = \frac{\alpha(M_Z)}{\pi} \frac{m_t^2}{M_Z^2} - \frac{\alpha(M_Z)}{4\pi} \ln \frac{m_H^2}{M_Z^2}$

$$g_{Vf}/g_{Af} = 1 - 2 \frac{2Q_f}{T_f^3} \sin\theta^f_{W,eff}$$

So $\mathcal{A}_f$ is directly related to $\sin\theta^f_{W,eff}$

$\mathcal{A}_f$ for different fermions

The actual $\mathcal{A}_f$ dependence on $\sin\theta^f_{W,eff}$ varies with the fermion charge and weak-isospin

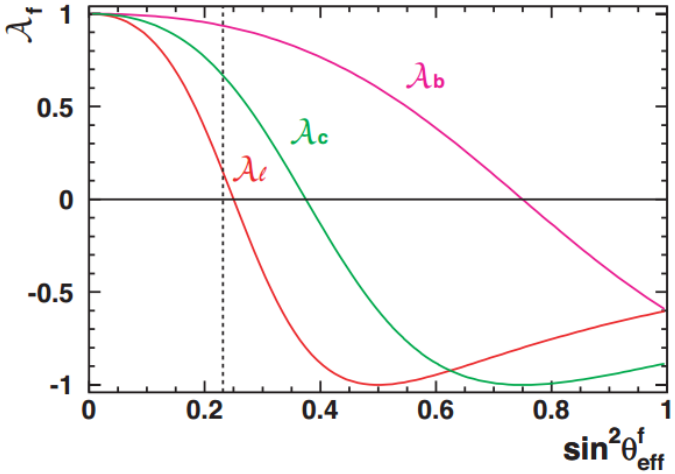

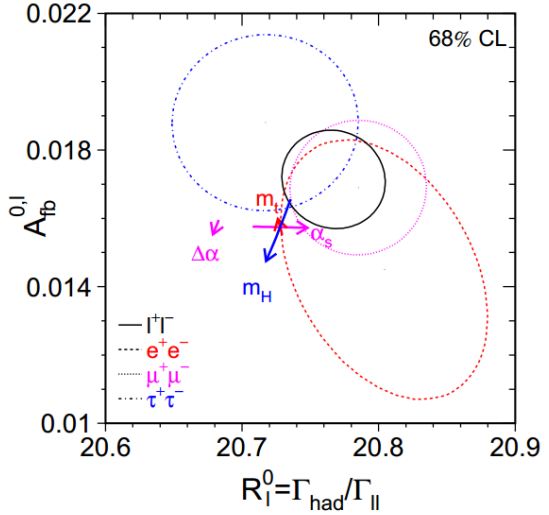

A_{FB}^{ℓ}: testing lepton universality

$$A_{FB}^{0,e} = 0.0145 \pm 0.025$$
$$A_{FB}^{0,\mu} = 0.0169 \pm 0.013$$
$$A_{FB}^{0,\tau} = 0.0188 \pm 0.017$$
$$A_{FB}^{0,\ell} = 0.0171 \pm 0.010$$

$A_{FB}^{0,e}$ suffers from uncertainties related to t-channel, as well as to s-t interference.

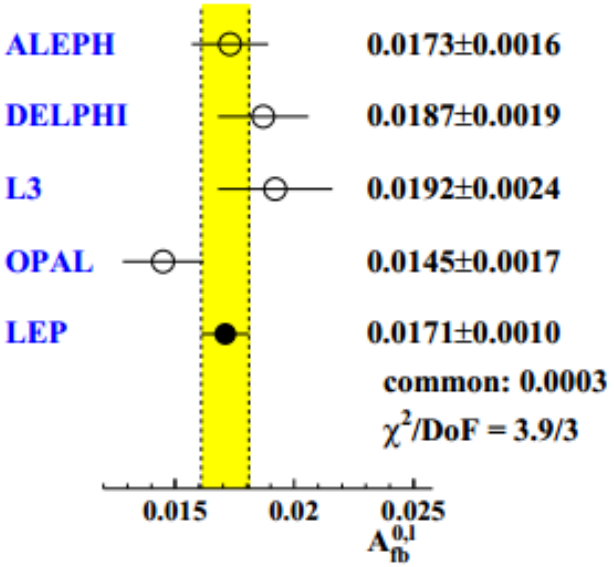
ALEPH
0.0173±0.0016
DELPHI
0.0187±0.0019
L3
0.0192±0.0024
OPAL
0.0145±0.0017
LEP
0.0171±0.0010
common: 0.0003
χ²/DoF = 3.9/3
0.015
0.02
0.025
A^0,l_fb

A_{FB} for quarks

Need to tag also the flavour and distinguish bc from $\bar{b}\bar{c}$, not only bc from q

Done only for $A_{FB}^{c\bar{c}}$ and $A_{FB}^{b\bar{b}}$ with different techniques:

- lifetime tagging;
  - $c\tau$ for b is $\sim 450\mu m$ (in lab $\times\gamma$)
  - $c\tau$ for c is $\sim 150\mu m$ (in lab $\times\gamma$)
  - detect displaced secondary vertex by impact parameter or decay lenght measurements
- Exclusive decays:
  - leptonic decay;
  - decay with D mesons;
- additional techniques:
  - jet charge;
  - vertex charge;
  - kaons;

Correction to asymmetries from QCD (gluon radiation from final state quarks), in addition to QED correction and LEP energy scale.

lifetime tagging

d_0 significance

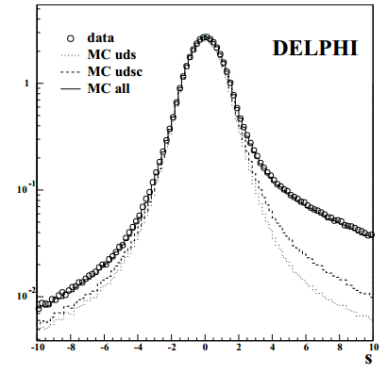

L significance and NN

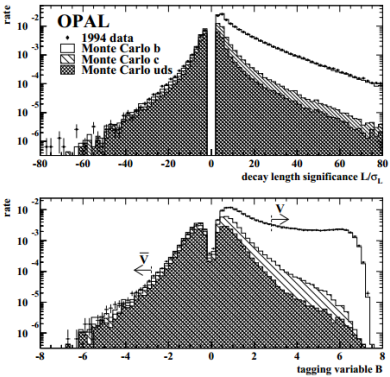

$b \leftrightarrow c$ separation via M_{vtx}

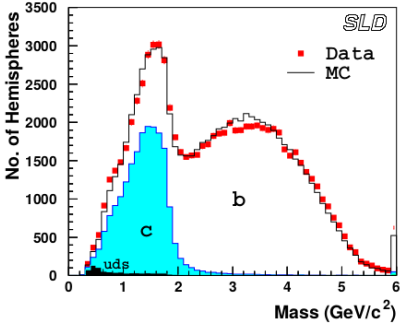

b-tagging performance

	ALEPH	DELPHI	L3	OPAL	SLD
b Purity [%]	97.8	98.6	84.3	96.7	98.3
b Efficiency [%]	22.7	29.6	23.7	25.5	61.8

Resolution

$\delta_{IP} \sim 16 - 100\mu m\ (R\phi/Z)$,
$\delta_b \sim 300\mu m$

Lepton tagging

A lepton inside a jet is a stong indication of a b or c flavour.

To distinguish from b to $\bar{b}$ use semileptonic decay of b quarks.

- $b \to \ell^-$; $\approx 10\%$
- $c \to \ell^+$; $\approx 13\%$
- $b \to c \to \ell^+$ cascade decay ;

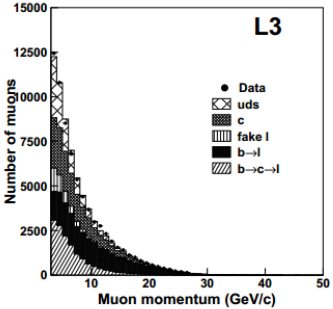

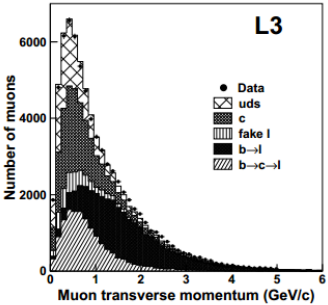

- Distinguish between direct and cascade decay using lepton p_T and p
- lower purity and efficiency wrt lifetime tagger

D-Meson Tags

Tagging via reconstruction of charmed meson and barions in jet:

direct evidence of a jet originated by an heavy quark.

- low $\mathcal{B} \sim \mathcal{O}(\%)$
- $b \to c$ fragmentation is small
- distinguish c from b decay by charmed mesons momentum;
  - $D_0 \to K^- \pi^+$
  - $D_+ \to K^- \pi^+ \pi^+$
  - $D_s \to K^+ K^- \pi^+$
  - $\Lambda_c^+ \to p K^- \pi^+$
  - $D^{*+} \to \pi^+ D^0$
    - slow π^+, no need for PID

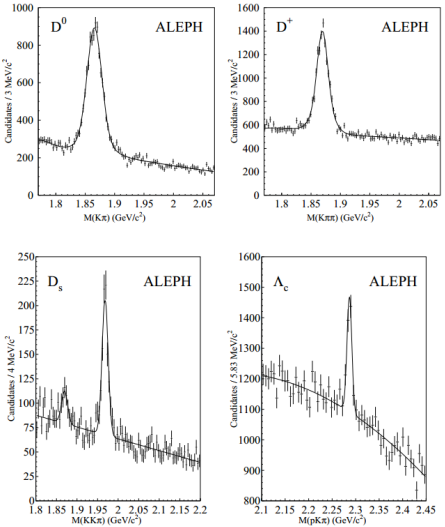

Jet charge, vertex charge and kaons

Consider $ee \to q\bar{q} \to jet + jet$ events.
The **average charge of all particles within a jet** retains some info about initial q charge.

$$Q_h = \frac{\Sigma_i q_i p_{i\parallel}^k}{\Sigma_i p_{i\parallel}^k}$$

where $p_{i\parallel}^k$ is the p parallel to trust axis of the event (corresponding to jets' directions)

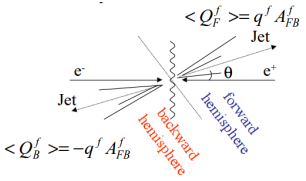

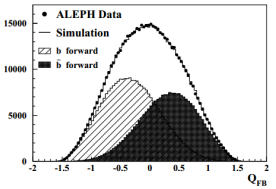

Likewise, the sum can run over all the **charged particles from a secondary (displaced) vertex**.
Tag efficieny is rather small: data driven estimation from fraction of same-sign double tag in pure sample of q quarks.

Kaons: deduce the q flavour via decay chain $b \to c \to s$ and $c \to s$

A_{FB} for b and c

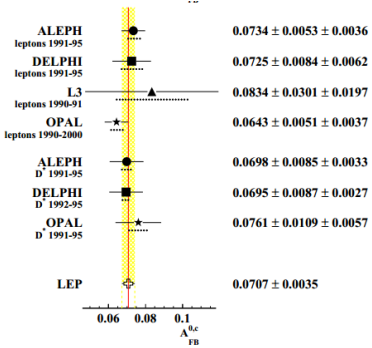

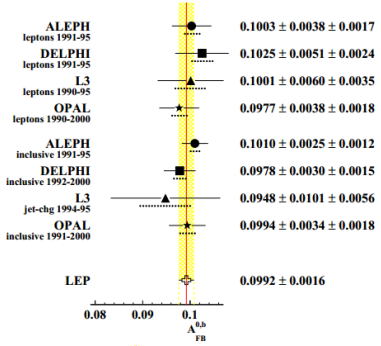

$$A_{FB}^{0,c} = 0.0707 \pm 0.0035$$

$$A_{FB}^{0,b} = 0.0992 \pm 0.0016$$

Note that $A_{FB}^{0,b/c}\left(\propto (\mathcal{A}_e \mathcal{A}_{b/c})\right) > A_{FB}^{0,\ell}\left(\propto (\mathcal{A}_e \mathcal{A}_\ell)\right)$, since $g_V^{b/c} > g_V^{\ell}$

Dotted line is syst error

A_{FB} for b and c vs $\sqrt{s}$

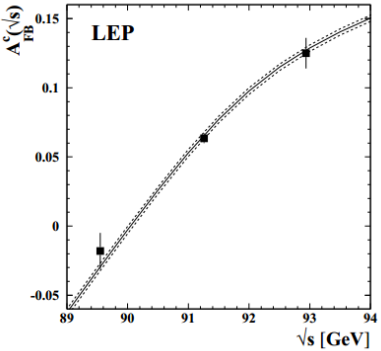

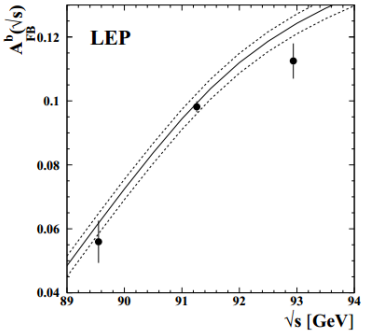

Note larger error off-peak: contribution from s/t interference term

Inclusive Hadronic Charge Asymmetry

Do not try to distinguish between quark flavour, but rather measure an "average" asymmetry based on charge asymmetries.

$$\langle Q_{FB}^{had} \rangle = \langle Q_F - Q_B \rangle = \sum_{q=udcsb} R_f A_{FB}^f \delta_q$$

$\delta_q = \langle Q_q - Q_{\bar{q}} \rangle$ jet charge diff for $q\bar{q}$

$\langle Q_{FB}^{had} \rangle$ can be interpreted as a function of $\sin^2\theta_{eff}^{lept}$ (in A_{FB}^f)

δ_q from $Z \to bb/cc$ and MC for udc (large syst uncert)

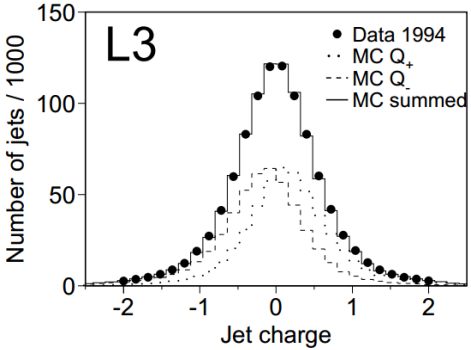

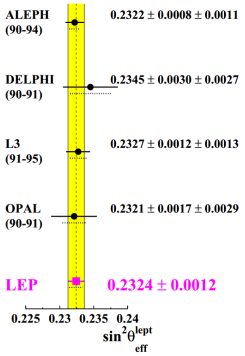

Left-Right Asymmetries

- The forward-backward asymmetry is due to the presence of axial and vector couplig of fermions in the neutral current, introducing a dependence on $\cos\theta$ which can be measured.
- Z coupling to left and right fermions are different as well, since L and R fermions belongs to different multiplet in the SM, with different quantum numbers.
- This feature can be measured studing the Z production with polarized $e^{\pm}$ beam, or by looking at the polarization of the decay product of the Z.
  - SLD produces Z with polarized $e^{\pm}$ beams;
    - Most precise determination of $\mathcal{A}_e$
  - LEP measure the polarization of τ in $Z \to \tau\tau$ decay, studing subsequent τ decays;

Differential x-section for polarized beam

For unpolarized beam

$$\frac{d\sigma}{d\cos\theta} \propto (1+\cos^2\theta) + \mathcal{A}_e\mathcal{A}_f 2\cos\theta$$

Differential cross section (born-level) in case of initial- or final-state fermion helicity are:

$$\frac{d\sigma_{Ll}}{d\cos\theta} \propto g_{Le}^2 g_{lf}^2 (1+\cos\theta)^2 + f(\mathcal{A}_{e,f})\cos\theta$$
$$\frac{d\sigma_{Rr}}{d\cos\theta} \propto g_{Re}^2 g_{rf}^2 (1+\cos\theta)^2 + \dots$$
$$\frac{d\sigma_{Lr}}{d\cos\theta} \propto g_{Le}^2 g_{rf}^2 (1-\cos\theta)^2 + \dots$$
$$\frac{d\sigma_{Rl}}{d\cos\theta} \propto g_{Re}^2 g_{lf}^2 (1-\cos\theta)^2 + \dots$$

LR is the helicity of initial state electron, *lr* is the helicity state of final-state fermion

For e^- with partial polarization $\mathcal{P}_e$ and e^+ unpolarized (SLC), summing over final-state polarization

$$\frac{d\sigma_{f\bar{f}}}{d\cos\theta} = \frac{3}{8}\sigma_{f\bar{f}}^{tot}\left[(1-\mathcal{P}_e\mathcal{A}_e)(1+\cos^2\theta)+2(\mathcal{A}_e-\mathcal{P}_e)\mathcal{A}_f\cos\theta\right]$$

$\mathcal{P}_e$ is positive for right-handed beam helicity, negative for left.

Measurements (see also next slides)

- if we look at total x-section for left/right-polarized e^- beam:
  - $\sigma_{L/R}^{tot}$ sensitive to $(1+\cos^2)$ term:
  - A_{LR} sensitive to $\mathcal{A}_e$
- if we look at forward/backward x-section for left/right-polarized e^- beam:
  - $\sigma_{L/R}^{F/B}$ sensitive to $\cos\theta$ term:
  - A_{LRFB} sensitive to $\mathcal{A}_f$
- A_{FB} sensitive to $\mathcal{A}_e\mathcal{A}_f$

- Measure the x-section for $e_L^- e^+ \to f\bar{f}$ (σ_L^f)
- and $e_R^- e^+ \to f\bar{f}$ (σ_R^f).
  - Note: only e^- beam is polarized;
  - the polarization is not complete $\mathcal{P}_e \sim 0.8$
  - $\mathcal{P}_e > 0$ for Left, $\mathcal{P}_e < 0$ for Right electrons;
  - Final state is inclusive, no flavour determation needed;

$$A_{LR} = \frac{\sigma_L^f - \sigma_R^f}{\sigma_L^f + \sigma_R^f}$$

From A_{LR} get $\mathcal{A}_e$from $(1 + \cos^2\theta)$ term integration:

$$\sigma_{L/R}^f = \int_{-1}^{+1} \frac{d\sigma_L}{d\cos\theta} d\cos\theta \propto 1 \pm \mathcal{P}_e \mathcal{A}_e$$

$$A_{LR} = \frac{N_L^f - N_R^f}{N_L^f + N_R^f} \frac{1}{\langle |\mathcal{P}_e| \rangle} = \mathcal{A}_e$$

NB. by comparison: $A_{FB}^0 = \frac{3}{4}\mathcal{A}_e\mathcal{A}_f$

It is also possible to combine the two techniques: FB and LR.

$$A_{LRFB} = \frac{(\sigma_F - \sigma_B)_L - (\sigma_F - \sigma_B)_R}{(\sigma_F + \sigma_B)_L + (\sigma_F + \sigma_B)_R}$$

The integration to get $_F$ and $_B$ drop the $(1 + \cos^2\theta)$ term and keep the $\cos\theta$ one.
$\sigma_{F/B} \propto (\mathcal{A}_e \mp \mathcal{P}_e)\mathcal{A}_f$,
$(\sigma_F - \sigma_B)_{L/R} \propto (\mathcal{P}_e)\mathcal{A}_f$

$$A_{LRFB} = \frac{(N_F - N_B)_L - (N_F - N_B)_R}{(N_F + N_B)_L + (N_F + N_B)_R} \frac{1}{\langle|\mathcal{P}_e|\rangle} = \frac{3}{4}\mathcal{A}_f$$

Possible to measure directly $\mathcal{A}_f$ for identified final state ($f = e, \mu, \tau, b, c$)
In both case, the precise knowledge of $\mathcal{P}_e$ is critical

SLC: beam polarization [3]

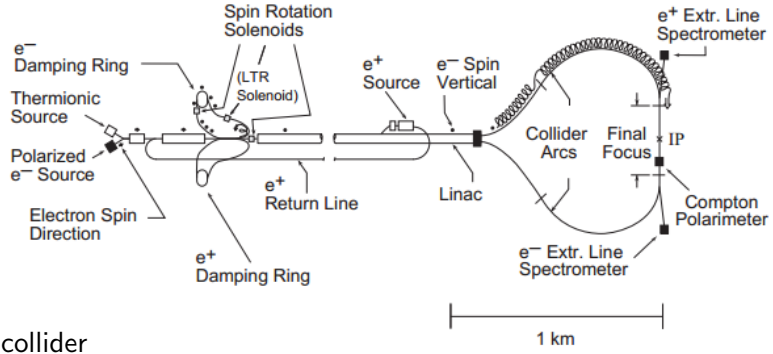

First $e^{\pm}$ linear collider

- e^- source
  - polarized by shining circ. polarized light on a ArGa photo-cathode ($\mathcal{P}_e \sim 22\%$)
  - then "strained lattice" photo-cathode ($\mathcal{P}_e \sim 80\%$);
  - polarization rotated to horizontal and then vertical pol;

SLC: beam polarization [3]

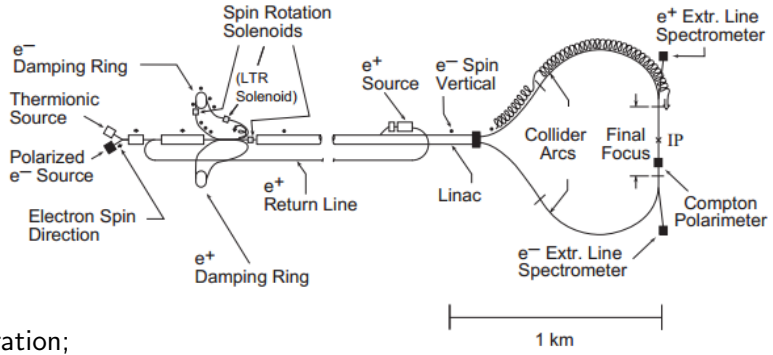

- linear acceleration;
  - e^+ produced by e^- on a target, and collected, squized and accelerated;
- two damping rings to reduce size and energy spread of $e^\pm$ bunches;
- final arch to single interaction region 1 GeV lost for sync. rad.
  - spin further rotated, and collision with longitudinal pol.
- repetition rate 120 Hz (45 o 90 kHz at LEP)
- Polarization randomly rotated every pulse (120 Hz) by changing the laser circ pol

$\mathcal{P}_e$ measured continously via a downstream Compton polarimeter [4, 5]

- Compton scattering is senstitive to $\mathcal{P}_e$ and $\mathcal{P}_\gamma$ ($\sigma(j = 3/2) > \sigma(j = 1/2)$)
- maximum for "head-on" $\gamma - e$ collisions
- High intensity laser (25MW), lead to 1000 compton interaction per pulse
- Compton-scattered e^- are bent by a magnet and analyzed by multichannel cherenkov detector
- Compton-scattered γ are analyzed by a quarz-fiber calorimeter for cross-check

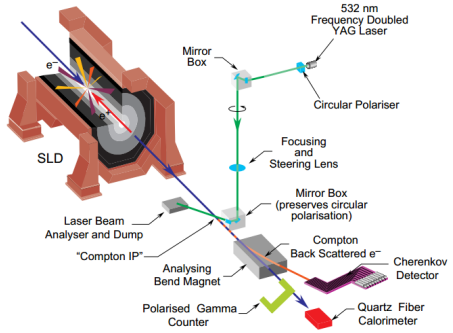

Electron polarization durin data-taking

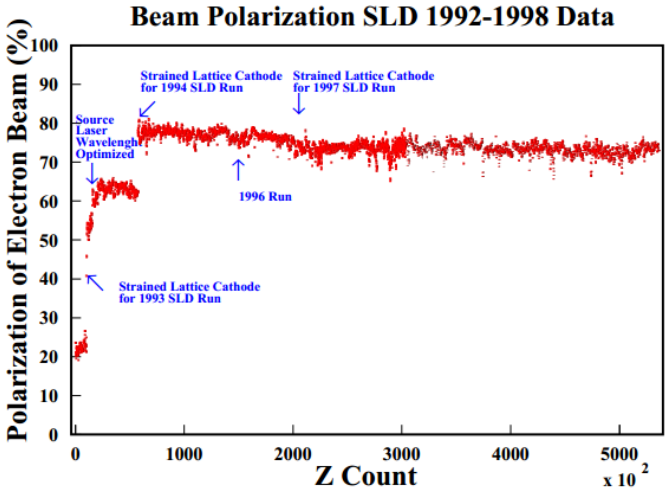

$\sigma_{\mathcal{P}_e} \sim 0.5\%$ (initial 2.7%)

Energy calibration

- $\sqrt{s}$ at SLC was measured and monitored downstream of the beams;
- precise vertical bending dipole to bend the beam;
- two horizontal bending magnets to produce synchrotron radiation before and after dipole;
- syncrotron light monitor to measure the bending;
- Expected precision 20 *MeV*
- Absolute calibration from Z peak mass and comparing with LEP results
  - At LEP $\sigma(\sqrt{s}) \approx 1.7\,\text{MeV}$ (100 keV w/o tidal effect)

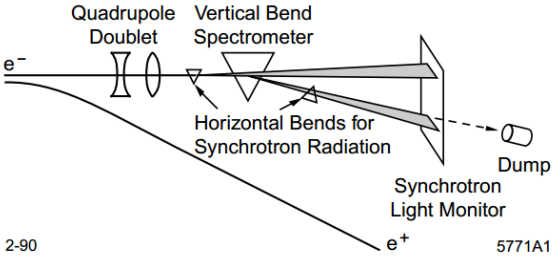

SLDetector

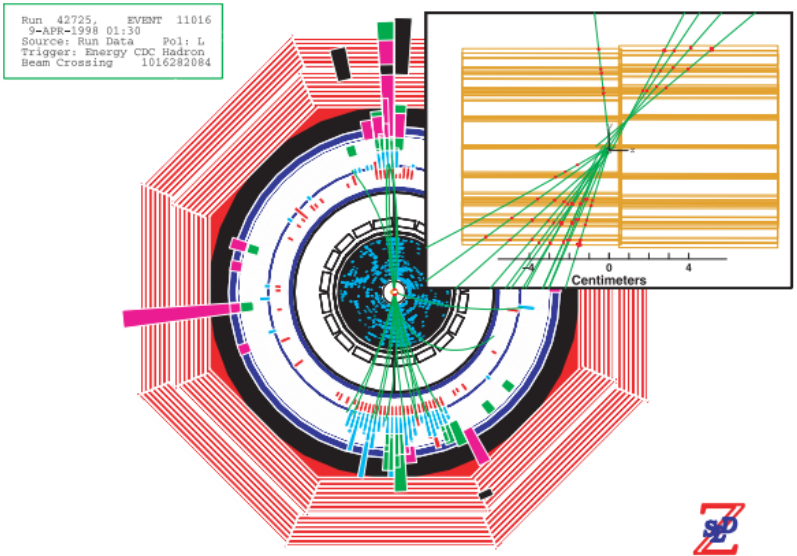

- Beam pipe (and beam) smaller than LEP, closer vertex detector;
- Slow repetition rate, use slow but high resolution CCD arrays;
- Central Drift Chamber
- LAr calorimeter

Event selection as at LEP, better b/c tagging.

$$A^0_{LR} = 0.1514 \pm 0.0022$$

- syst. uncert:
  - $\delta\mathcal{P}_e/\mathcal{P}_e \sim 0.5\%$
  - interference correction (0.39%)
  - $\sqrt{s}$ (0.15%)
- Additional asymmetries (arc spin trasport, e^+ polarization, lumi) negligible

$$A^0_{LR} = \frac{2(1-4\sin^2\theta^{lept}_{eff})}{1+(1-4\sin^2\theta^{lept}_{eff})}$$

$$\sin^2\theta^{lept}_{eff} = 0.23097 \pm 0.00027$$

at LEP

$$\sin^2\theta^{lept}_{eff} = \pm.00043$$

SLC 0.5M $Z \to ff$ vs LEP 15M $Z \to q\bar{q}$ plus 1.7M $Z \to \ell\ell$

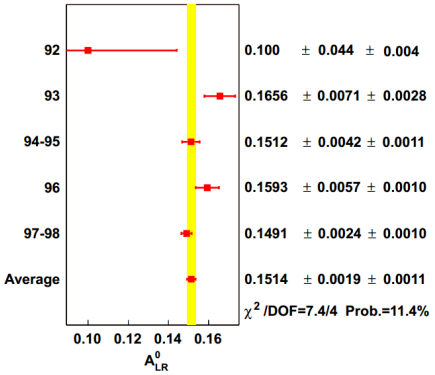

- Computed for $\ell = e, \mu, \tau$
  - 15k $Z \to ee$, 12k $\to \mu\mu$, 11k $\to \tau\tau$
  - via likelihood fit to $\frac{d}{d\cos\theta}$
  - uncertainties dominated by statistics
  - then radiative corrections, polarization, background
- larger for τ due to τ decay ID
- smaller for e: from A_{LR} and A_{LRFB}

$$\mathcal{A}_e = 0.1544 \pm 0.0060$$
$$\mathcal{A}_\mu = 0.142 \pm 0.015$$
$$\mathcal{A}_\tau = 0.136 \pm 0.025$$
$$\mathcal{A}_\ell = 0.1513 \pm 0.0021,\ \sin^2\theta^{lept}_{eff} = 0.23098 \pm 0.00026$$

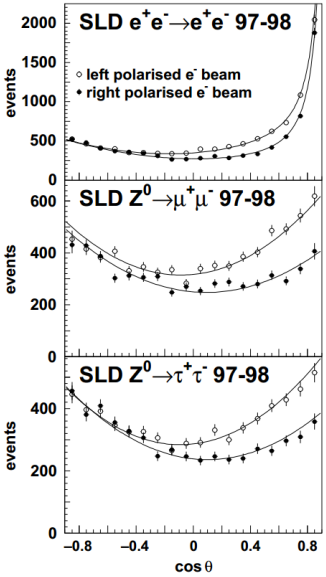

τ polarization

- At LEP $e^{\pm}$ not polarized, but it is possible to look at the polarization of final state in $Z \to \tau\tau$ decays, by using the $\tau \to \nu_\tau + X$ decay.

$$\mathcal{P}_\tau = \frac{\sigma_+ - \sigma_-}{\sigma_+ + \sigma_-}$$

where σ_+ is the x-sec to produce positive helicity τ^- etc.

- Must take care that τ have mass, so helicity state do not correspond to chirality state (the one involved directly in the SM coupling).
  - However at LEP, $p_\tau \approx M_Z/2 \gg m_\tau$, so helicity $\approx$ chirality

$$\mathcal{P}_\tau = -\frac{\mathcal{A}_\tau(1+\cos^2\theta_{\tau^-}) + 2\mathcal{A}_e\cos\theta_{\tau^-}}{(1+\cos^2\theta_{\tau^-}) + 8/3 A_{FB}^\tau \cos\theta_{\tau^-}}$$

- Can derive $\mathcal{A}_e$ and $\mathcal{A}_\tau$

Experimental method

- Consider $\tau \to \pi\nu$ decay.
- It is purely V-A charged weak current, and obviously conserve angular momentum. In the τ rest frame, the neutrino (LH) is emitted opposite to τ spin, and so the π is emitted backward, namely along the τ spin.

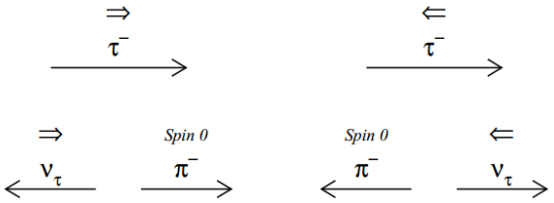

- If the τ has positive helicity (spin $\parallel$ to momentum) then the π is emitted in the p_τ direction (left configuration), and so, in the LAB (LEP CM), has larger momentum.
- If helicity is negative (spin anti$\parallel$), π is emitted in opposite direction and has smaller momentum.
- Bottomline: if τ has positive (negative) helicity, the π momentum is higher (lower)

(a) Measure the direction of π in the τ rest frame $\cos\theta_\pi$

$$\frac{1}{\Gamma}\frac{d\Gamma}{d\cos\theta_{pi}} = \frac{1}{2}(1 + \mathcal{P}_\tau \cos\theta_\pi)$$

boosted in the LAB ($x_\pi = E_\pi/E_\tau = E_\pi/E_{beam}$)

$$\frac{1}{\Gamma}\frac{d\Gamma}{dx_{pi}} = 1 + \mathcal{P}_\tau(2x_\pi - 1)$$

Similar, but more complex, and less sensitive, for

(b) $\tau \to \rho\nu$

(c) $\tau \to a_1\nu$

(d) $\tau \to \mu(e)\nu\nu$

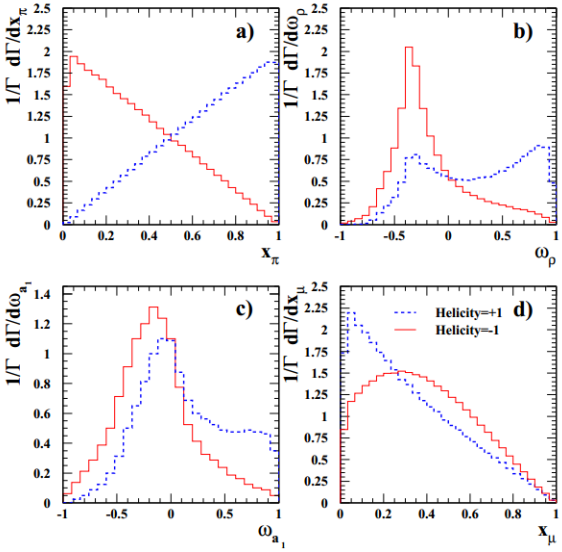

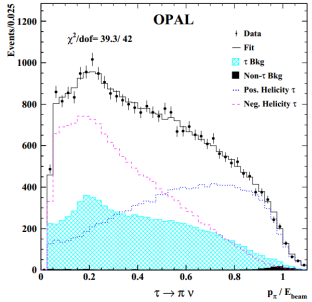
OPAL
χ^2/dof= 39.3/ 42
Data
Fit
τ Bkg
Non-τ Bkg
Pos. Helicity τ
Neg. Helicity τ
Events/0.025
$\tau \to \pi \nu$
p_π / E_{beam}

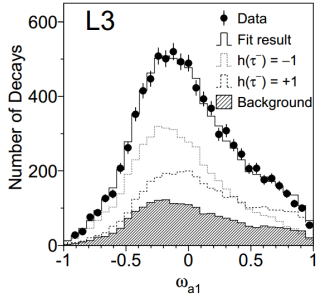
L3
Data
Fit result
h(τ⁻) = −1
h(τ⁻) = +1
Background
Number of Decays
ω_{a1}

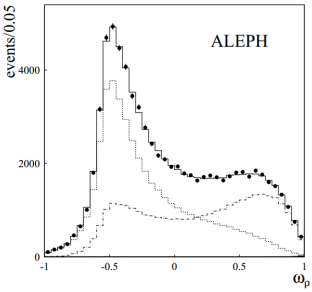
ALEPH
events/0.05
ω_ρ

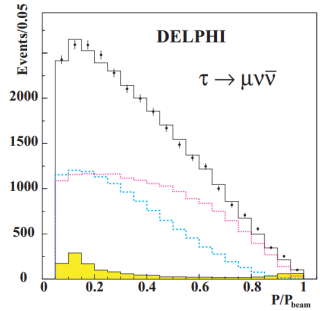
DELPHI
$\tau \to \mu\nu\overline{\nu}$
Events/0.05
P/P_{beam}

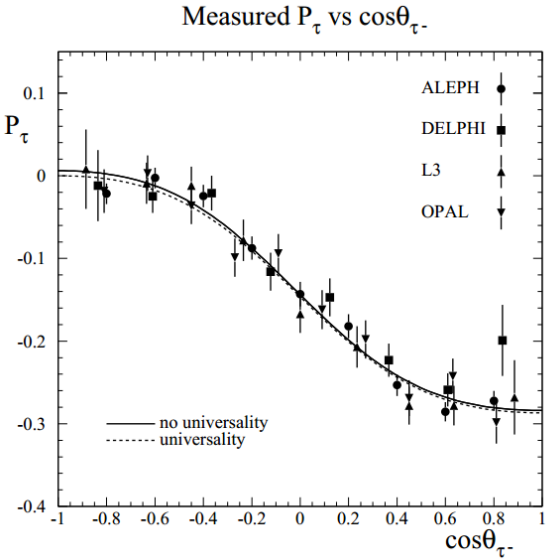

$$\mathcal{A}_\tau = 0.1439 \pm 0.0043$$
$$\mathcal{A}_e = 0.1498 \pm 0.0049$$

$$\mathcal{A}_\ell = 0.1465 \pm 0.0033$$
$$\sin^2\theta^{lept}_{eff} = 0.23159 \pm 0.00041$$

Results on axial and vector coupling

g^f_{V-A} scale from $\sigma_{ff} \propto g^2_{Vf} + g^2_{Af}$

g^f_{V-A} ratio from $\mathcal{A}_f = 2\frac{g_{Vf}/g_{Af}}{1+(g_{Vf}/g_{Af})^2}$

$$A^0_{FB} = \frac{3}{4}\mathcal{A}_e\mathcal{A}_f$$

$$A^0_{LR} = \mathcal{A}_e$$

$$A^0_{LRFB} = \frac{3}{4}\mathcal{A}_f$$

$$\mathcal{P}_\tau = -\mathcal{A}_\tau$$

Results on axial and vector coupling

g^f_{V-A} scale from $\sigma_{ff} \propto g^2_{Vf} + g^2_{Af}$

g^f_{V-A} ratio from $\mathcal{A}_f = 2\frac{g_{Vf}/g_{Af}}{1+(g_{Vf}/g_{Af})^2}$

$$A^0_{FB} = \frac{3}{4}\mathcal{A}_e\mathcal{A}_f$$
$$A^0_{LR} = \mathcal{A}_e$$
$$A^0_{LRFB} = \frac{3}{4}\mathcal{A}_f$$
$$\mathcal{P}_\tau = -\mathcal{A}_\tau$$

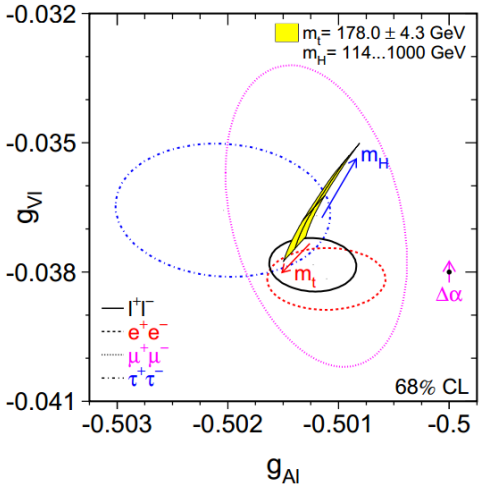

Results on axial and vector coupling

g^f_{V-A} scale from $\sigma_{ff} \propto g^2_{Vf} + g^2_{Af}$

g^f_{V-A} ratio from $\mathcal{A}_f = 2\frac{g_{Vf}/g_{Af}}{1+(g_{Vf}/g_{Af})^2}$

$$A^0_{FB} = \frac{3}{4}\mathcal{A}_e\mathcal{A}_f$$

$$A^0_{LR} = \mathcal{A}_e$$

$$A^0_{LRFB} = \frac{3}{4}\mathcal{A}_f$$

$$\mathcal{P}_\tau = -\mathcal{A}_\tau$$

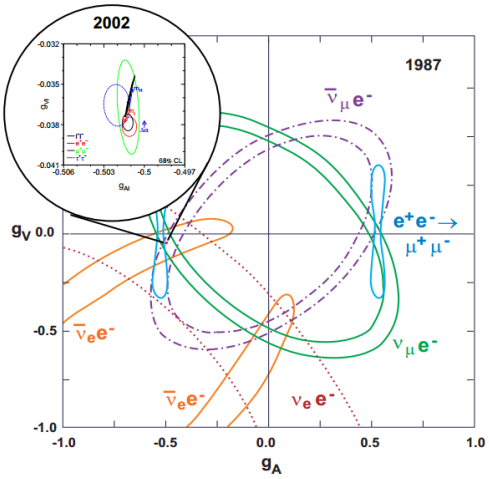

C and B quarks coupling

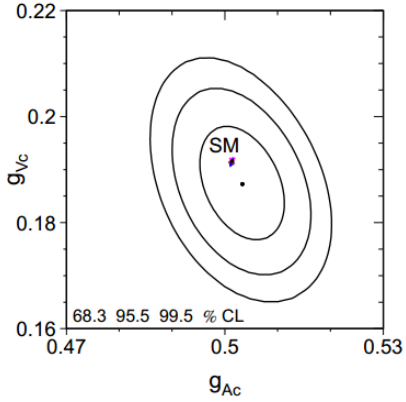

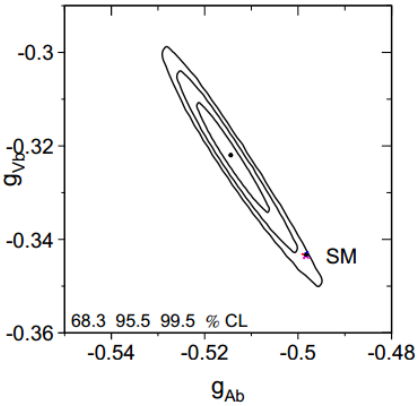

$A_{FB}^{0,b} \propto \mathcal{A}_b \propto g_V^b g_A^b$ (anticorrelation between g_V^b and g_A^b)

Off by 2.6σ wrt SM global fit

$\mathcal{A}_q$vs $\mathcal{A}_\ell$

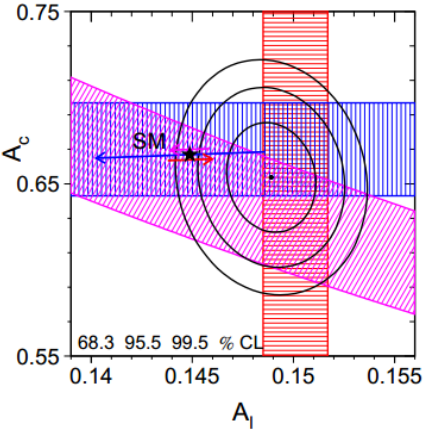

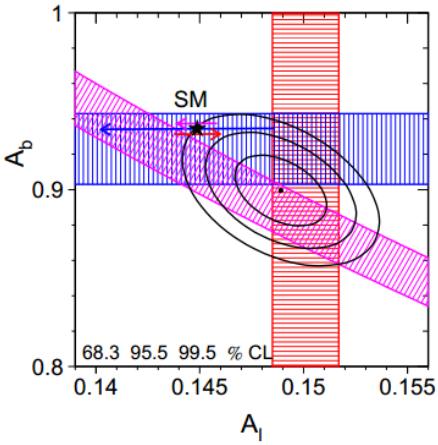

vert band: $\mathcal{A}_\ell$, horiz: $\mathcal{A}_q$, diagonal: $A_{FB}^{0,q}$

$\sin^2\theta^{lept}_{eff}$

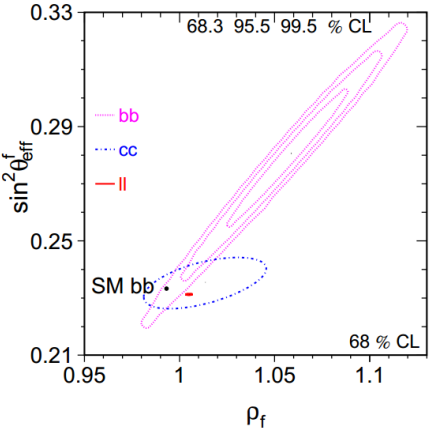

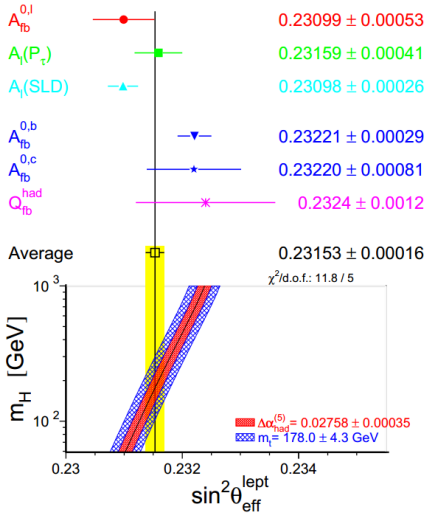

Input to global EWK fit

(in parenthesis the order followed in these lessons)

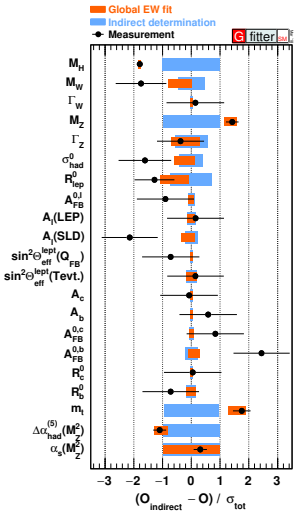

- Higgs mass (4)
  - LHC
- W mass and width (2)
  - LEP2, Tevatron, LHC
- Z-pole observables (1)
  - LEP1, SLD
  - M_Z, Γ_Z
  - σ_0^{had}
  - $\sin^2\theta^{lept}_{eff}$
  - Asymmetries
  - BR $R^0_{lep,b,c} = \Gamma_{had}/\Gamma_{\ell\ell,b\bar{b},c\bar{c}}$
- Top mass (3)
  - Tevatron, LHC
- other:
  - $\alpha_s(M_Z^2)$, $\Delta\alpha_{had}(M_Z^2)$

Input to global EWK fit
(in parenthesis the order followed in these lessons)

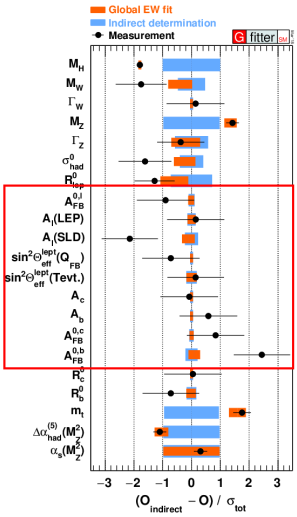

- Higgs mass (4)
  - LHC
- W mass and width (2)
  - LEP2, Tevatron, LHC
- Z-pole observables (1)
  - LEP1, SLD
  - M_Z, Γ_Z
  - σ^{had}_0
  - $\sin^2\theta^{lept}_{eff}$
  - Asymmetries
  - BR $R^0_{lep,b,c} = \Gamma_{had}/\Gamma_{\ell\ell,b\bar{b},c\bar{c}}$
- Top mass (3)
  - Tevatron, LHC
- other:
  - $\alpha_s(M^2_Z)$, $\Delta\alpha_{had}(M^2_Z)$

ALEPH, DELPHI, L3, OPAL, SLD, LEP Electroweak Working Group, SLD Electroweak Group, SLD Heavy Flavour Group Collaboration, S. Schael *et al.*, "Precision electroweak measurements on the Z resonance," *Phys.Rept.* **427** (2006) 257–454, arXiv:hep-ex/0509008 [hep-ex].

F. Halzen and A. D. Martin, *Quarks and Leptons: an introductory course in modern particle physics*. Wiley, New York, USA, 1984.

G. A. Loew, "The slac linear collider and a few ideas on future linear colliders," *Proceedings of the 1984 Linear Accelerator Conference* (1984) . https://inis.iaea.org/search/search.aspx?orig_q=RN:16018252.

G. Shapiro, S. Bethke, O. Chamberlain, R. Fuzesy, M. Kowitt, D. Pripstein, B. Schumm, H. Steiner, M. Zolotorev, P. Rowson, D. Blockus, H. Ogren, M. Settles, M. Fero, A. Lath, D. Calloway, R. Elia, E. Hughes, T. Junk, and G. Zapalac, "The compton polarimeter at the slc,". https://escholarship.org/uc/item/78t2f6wp.

SLD Collaboration, M. J. Fero, "The Compton polarimeter for SLC," in *Frontiers of high energy spin physics. Proceedings, 10th International Symposium, 35th Yamada Conference, SPIN'92, Nagoya, Japan, November 9-14, 1992*, pp. 899–904. 1992. http://www-public.slac.stanford.edu/sciDoc/docMeta.aspx?slacPubNumber=SLAC-PUB-6026.

Outline

Outline

Outline

Outline